The Journal of Neuroscience, September 15, 1996, *16*(18):5777–5794

Distribution of Networks Generating and Coordinating Locomotor Activity in the Neonatal Rat Spinal Cord *In Vitro*: A Lesion Study

Ole Kjaerulff and Ole Kiehn

Division of Neurophysiology, Department of Medical Physiology, The Panum Institute, University of Copenhagen, DK-2200 Copenhagen, Denmark

The isolated spinal cord of the newborn rat contains networks that are able to create a patterned motor output resembling normal locomotor movements. In this study, we sought to localize the regions of primary importance for rhythm and pattern generation using specific mechanical lesions. We used ventral root recordings to monitor neuronal activity and tested the ability of various isolated parts of the caudal thoracic-lumbar cord to generate rhythmic bursting in a combination of 5-HT and NMDA. In addition, pathways mediating left/right and rostrocaudal burst alternation were localized. We found that the isolated ventral third of the spinal cord can generate normally coordinated rhythmic activity, whereas lateral fragments resulting from sagittal sections showed little or no rhythmogenic capability compared with intact control preparations. The ability to generate fast and regular rhythmic activity decreased in the caudal direction, but the rhythm-generating network was found to be distributed over the entire lumbar region and to extend into the caudal thoracic region. The pathways mediating left/right alternation exist primarily in the ventral commissure. As with the rhythmogenic ability, these pathways were distributed along the lumbar enlargement. Both lateral and ventral funiculi were sufficient to coordinate activity in the rostral and caudal regions. We conclude that the networks organizing locomotor-related activity in the spinal cord of the newborn rat are distributed.

Key words: 5-HT; NMDA; neonatal rat; spinal cord; locomotion; central pattern generator

The ability of spinalized vertebrates to show purposeful rhythmic motor behaviors such as walking, swimming, or scratching is now recognized as a general phenomenon. The spinal neuronal networks, capable of generating and shaping the rhythmic motor activity also in the absence of movement-related sensory feedback, have been named central pattern generators (CPGs) (Delcomyn, 1980; Grillner, 1981).

In an attempt to circumvent the complexity of the mammalian nervous system, it seems reasonable to search for spinal cord regions where primary elements of the CPG might accumulate. One way of mapping the networks engaged in rhythmic actions is to label or monitor ensembles of cells depending on the intensity of neuronal activity. These principles underlie investigations using c-*fos* expression in the cat (Dai et al., 1990; Barajon et al., 1992), 2-deoxyglucose in the rabbit (Viala et al., 1988), and calcium imaging in chick embryos (O'Donovan et al., 1994). In general, these studies have pointed toward ventral and intermediate areas as being important for the generation of spinal rhythmic activity. Using activity-dependent labeling with the fluorescent dye sulforhodamine 101 in the *in vitro* neonatal rat preparation, we have previously presented a first attempt to localize the population of neurons generating locomotor-like activity in the rat (Kjaerulff et al., 1994). After chemically induced locomotor-like activity, we found consistent sulforhodamine labeling in the medial intermediate gray matter and close to the central canal. Although these observations are in accordance with previous observations obtained in studies using activity-dependent labeling and calcium imaging, they do not discriminate between areas that contain the CPGs for locomotion and areas containing neurons that are passively driven by the CPGs. Until now, this problem has generally limited the interpretation of such studies.

As a more direct alternative to the use of activity-dependent labeling or calcium imaging, specific lesions have been used to elucidate the organization of networks engaged in hindlimb rhythmic activity (Grillner and Zangger, 1979; Deliagina et al., 1983; Kudo and Yamada, 1987; Mortin and Stein, 1989; Cowley and Schmidt, 1993; Ho and O'Donovan, 1993; Wheatley et al., 1994). The majority of these studies has suggested that the network involved in locomotion is distributed along the rostrocaudal axis of the cord and that the potential for rhythm and pattern genesis is higher in rostral than in caudal segments. Recently, in the newborn rat, Cazalets et al. (1995) have advocated that the network responsible for generating locomotor-related rhythmicity is highly localized and that the spinal network organizing rhythmic activity is located only between the segments Th13 and L2.

Here, we present results from a lesion study, which show that networks ventral to the level of the central canal can generate normally coordinated rhythmic activity and that important CPG elements are more likely to be concentrated medially than laterally. Furthermore, rhythm and pattern generation are not restricted to one or two rostral lumbar segments, but extend to more caudal lumbar segments and to thoracic segments as well.

Part of this work has been presented previously in abstract form (Kjaerulff and Kiehn, 1994, 1995).

Received Jan. 17, 1996; revised June 17, 1996; accepted June 20, 1996.

This work was supported by the NOVO Foundation, the Carlsberg Foundation, and the Danish Medical Research Council. O.K. is a Hallas-Møller Senior Research Fellow. We thank Ingrid Kjaer and Conni Temdrup for technical assistance.

Correspondence should be addressed to Dr. Ole Kiehn, Division of Neurophysiology, Department of Medical Physiology, The Panum Institute, Blegdamsnvej 3, DK-2200 Copenhagen, Denmark.

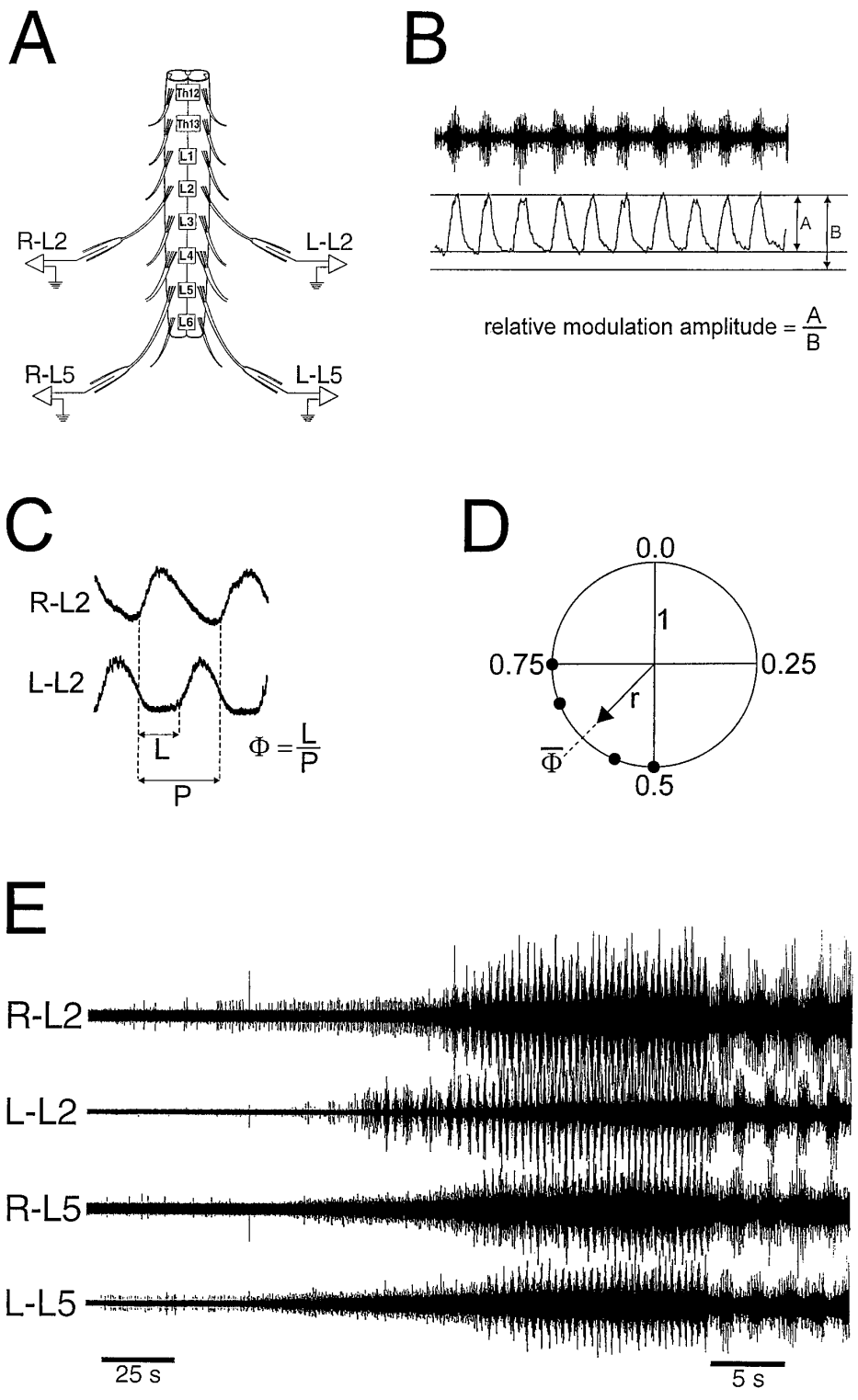

Figure 1. *A*, Experimental setup used to characterize left/right and rostrocaudal coordination patterns. Ventral root recordings were made from the right (*R*) and left (*L*) side both at the L2 and L5 level. *B*, Determination of the relative modulation amplitude. Ten ventral root cycles were full-wave-rectified and smoothed with low-pass filtering (time constant 200 msec), and the relative modulation amplitude was obtained from the mean peak (designated by *B*) and mean trough amplitudes (designated by *A*). *C*, Schematic showing how the phase values (Φ) were calculated from the period (*P*) and the latency (*L*). Records from right and left L2 ventral roots were full-wave-rectified and smoothed with low-pass filtering, and the right ventral root served as the reference recording. *D*, Circular phase-diagram in which four phase values have been plotted. The mean phase value($\bar{\Phi}$) is indicated. *r* indicates the concentration of phase values around the mean. *r* ranges from 0 to 1 and can be represented graphically by the length of the vector (see Materials and Methods). *E*, Onset of rhythmic activity induced with a combination of 7.5 μM 5-HT and 7.5 μM NMDA in an intact Th12–L6 preparation. Note the faster time scale in the last part of the recording. Bursting was preceded by a steadily increasing tonic discharge in R-L2, R-L5, and L-L5, whereas L-L2 had an abrupt onset of rhythmicity. Bursts showed left/right alternation between corresponding roots on each side of the cord, and bursts in L2 alternated with bursts in the ipsilateral L5. This coordination pattern characterizes fast regular bursting induced by 5-HT and NMDA.

MATERIALS AND METHODS

Dissection and induction of rhythmic activity. The lesions were performed on isolated spinal cords of newborn Wistar rats generally 1 d old (range 0–2 d). The part of the spinal cord used in the experiments generally included the lower thoracic and all the lumbar segments. Th12–L6 preparations were used in the majority of cases (Fig. 1*A*), but in a few experiments Th11 or Th13 made the rostralmost segments. A varying number of sacral segments were also sometimes included. The animals were anesthetized with ether, quickly decapitated, and eviscerated. They were then transferred to a petri dish filled with oxygenated, ice-cold Krebs' solution. The dissecting solution was identical to that used later during the experiments (see below) except that 90% of the $CaCl_2$ had been substituted with an equimolar quantity of $MgSO_4$ to block muscular contractions and protect the tissue against calcium-induced neuronal damage. The entire spinal cord was exposed by a ventral laminectomy. The isolated spinal cord preparation was transferred to the recording chamber superfused with Krebs' solution containing (in mM): 118 NaCl, 4.69 KCl, 25 $NaHCO_3$, 1.18 KH_2PO_4, 1.25 $MgSO_4$, 2.52 $CaCl_2$, and 11 glucose. The solution was aerated with 95% O_2 and 5% CO_2, and the temperature was kept constant at 25 ± 1°C.

For recording, the ventral roots were cut and placed in suction electrodes. All recordings were bandpass-filtered (100–10,000 Hz), digitized, stored on a digital tape recorder (Biologic, DTR 1800), and printed on thermosensitive paper (Gould 4000, Ilford, UK).

Rhythmic activity was induced before and after the lesion, with a combination of NMDA (4.5–9.0 μM, Sigma, St. Louis, MO) and 5-hydroxytryptamine (5-HT; 4.5–30 μM, Sigma) added to the superfusing solution. This drug combination was chosen because in previous experiments (Kjaerulff et al., 1994) we found that it gives rise to stable and long-lasting rhythmic activity, as has been shown previously for the coapplication of 5-HT and *N*-methyl-D,L-aspartate (NMA) (Sqalli-Houssaini et al., 1993). Because we were generally interested only in the changes in rhythmic activity resulting from the lesions, we usually used just a single combination of 5-HT and NMDA concentrations after the lesion. In a few instances, however, more than one set of concentrations was used. At least one combination of 5-HT and NMDA concentrations found to elicit regular and lasting rhythmic activity before the lesion was used postlesioning.

The lesioning procedure. The lesions were done in the recording chamber, primarily with a vibrating tungsten needle (Ho and O'Donovan, 1993). Fine iridectomy scissors were used to open the pial surface before using the needle. Agar blocks were used to keep the preparation fixed during cutting. After the lesion, we routinely tested for the presence of ventral root responses to stimulation of the ventral descending tracts at the rostral end of the preparation.

The preparations were allowed to incubate for at least 30 min in normal Krebs' solution after the lesion, before reapplication of 5-HT and NMDA. A lesioned preparation was considered incapable of generating rhythmicity in the used concentration if no modulated root activity was observed after a 90 min exposure to the neurochemicals (i.e., at least 2 hr after the lesion).

Histological evaluation of the lesions. To determine the precise localization of lesions along the rostrocaudal axis, and to confirm their uniformity, the preparations were fixed after the experiment in 4% paraformaldehyde or in Bouin's fixative, dehydrated, embedded in paraffin, cut transversely, and stained with cresyl violet. Five histological sections, equally spaced, were obtained from the full rostrocaudal extent of the preparation. The distance between a fixed anatomical landmark and the lesion was measured, and the SD of the five measurements was divided by the average width of the sections to relate the precision to the size of the preparation. This ratio did not exceed 10% ($n = 10$ animals). When determining the localization of transverse sections, the border between two segments was defined as the area giving rise to the most rostral root filament of the caudal segment.

We did not attempt to assess in detail the extent of possible superficial tissue damage in conjunction with the lesions. In general, the cutting surface was continuous without obvious signs of superficial damage. During whole-cell recordings in similarly lesioned preparations, living neurons are found within a distance of 50–75 μm from the cut surface (Kiehn et al., 1995, 1996).

Measurement of parameters characterizing rhythmic activity. The cycle period, defined as the time interval between the burst onsets (*P* in Fig. 1*C*), was measured for 10 consecutive cycles before and after the lesion. Typically, in the beginning of an episode with rhythmicity, the cycle period quickly reached a minimum before slowly increasing again (cf. Sqalli-Houssaini et al., 1993). The period was measured shortly after it reached the minimum. As also reported by Sqalli-Houssaini et al. (1993), the period occasionally progressively decreased, until phasic activity was converted into tonic discharge. This problem could be overcome by reducing the concentration of the rhythm-inducing neurochemicals.

In evaluating the quality of locomotor activity, we also determined the modulation amplitude before and after the lesion was done. After performing the recordings in the intact preparation, the suction electrodes had to be removed from the ventral roots for lesioning and then remounted before recording again. This procedure was expected to change the recording geometry. Therefore, instead of measuring the absolute modulation amplitude, we determined the relative modulation amplitude, which gives a measure of the rhythmic burst amplitude compared with the general level of activity (Fig. 1*B*). If the lesion leaves the excitability of the motoneurons unchanged, the size of the modulation amplitude reflects the modulatory drive, i.e., the strength of the phasic excitatory and/or inhibitory input converging onto the motoneurons.

The determination of coupling strength using circular statistics. Some midline lesions severely affected the coupling between bursting on the two sides of the preparations. To determine whether coupling was totally abolished or only weakened in these cases, we used circular statistics (Zar, 1974; Batschelet, 1981). Twenty-five L-L2 burst onsets were selected at random from individual episodes of rhythmic activity using a random number generator from a standard software package. The phase values (Φ) of the 25 L-L2 burst onsets were calculated with regard to R-L2 onsets. The phase calculation was done as shown in Figure 1*C* by dividing the latency (*L*) between the L-L2 onset and the latest preceding R-L2 onset by the R-L2 period (*P*). The mean phase, $\bar{\Phi}$ of the individual phases, Φ_1 through Φ_{25}, was calculated using the formula:

$$\tan\bar{\Phi} = \frac{Y}{X}, \tag{1}$$

where

$$X = \frac{\sum_{i=1}^{n} \cos \Phi_i}{n} \tag{2}$$

and

$$Y = \frac{\sum_{i=1}^{n} \sin \Phi_i}{n}. \tag{3}$$

In Equations 2 and 3, n was 25, the number of cycles in the sample.

In Figures 4, 5, 6*B*, and 6*D*, the L-L2 phase values have been plotted on a circle representing the interval of possible phases from 0 to 1. The phase values 0 and 1 are equivalent and reflect synchrony, whereas 0.5 is equivalent to alternation. The mean phase $\bar{\Phi}$ is indicated by the direction of the vector originating from the center of the circle (this is illustrated for four phase values in Fig. 1*D*).

A measure, *r*, indicates the concentration of phase values around the mean and can be calculated using the formula:

$$r = \sqrt{X^2 + Y^2}. \tag{4}$$

r ranges from 0 to 1 and can be represented graphically by the length of the vector.

The following reasoning was used in the evaluation of the left/right coupling strength. If bursting on the two sides in a given preparation is strongly coupled, then phase values would be expected to be highly concentrated around the mean phase. Conversely, the distribution of phases should show maximal dispersion and be uniformly distributed on the circle if bursting on the two sides is independent, that is, if there is no coupling. Using Rayleigh's test (Zar, 1974), we determined whether the concentration *r* of phases around the mean was sufficiently high to state that coupling was still present after the lesion. The coupling was considered significant when Rayleigh's test resulted in a p value <0.05.

The left/right coordination pattern before the lesion was always alternation. After the lesion, alternation—corresponding to a mean phase of 0.5—was therefore the cardinal alternative hypothesis against independent bursting (corresponding to no mean phase). This opportunity to specify the mean phase in the alternative hypothesis increases the statistical power (i.e., preserved coupling after the lesion is more likely to be detected). A modified form of Rayleigh's test was used in this context (Zar, 1974).

The Watson–Williams test (Zar, 1974; Batschelet, 1981) was used to determine whether the coupling strength changed significantly after the lesion. This procedure implies a comparison of the concentration of phase values, *r*, before and after the lesion. For all statistical tests, 5% was chosen as the level of significance.

RESULTS

A rhythmic motor output could be induced chemically in all ($n = 55$) the control preparations. In 52 preparations (95%), this activity was regular and persistent, and was recorded generally in four, and at least in three, ventral roots. In the remaining three preparations, the activity was either short-lasting or was observed in one or two ventral roots only, making a comparison between

intact and lesioned preparations difficult. Hence, the results reported here are based on data from the first 52 animals.

Rhythmic activity in unlesioned control preparations

In most ventral root recordings, the first observation after the arrival of the rhythm-inducing neurochemicals to the recording chamber was a steadily increasing unmodulated discharge. This tonic activity ultimately reached a constant level and provided a permanent background for the rhythmic activity. Discernible bursting followed the onset of tonic activity after 2 ± 2 min (mean ± SD, $n = 45$ experiments) and developed fully into stable, high-amplitude rhythmic activity after a further delay of 3 ± 3 min. The typical gradual onset of rhythmicity is illustrated in Figure 1*E*, ventral roots R-L2, R-L5, and L-L5. In a minority of cases, the onset of rhythmicity was much more sudden and occurred concomitantly with the onset of tonic activity (Fig. 1*E*, *L-L2*).

The characteristic regular bursting recorded in L2 and L5 ventral roots in unlesioned control preparations is shown in Figure 1*E*. Left/right alternation is observed both at the L2 and the L5 level, and there is a rostrocaudal alternation between ipsilateral L2 and L5 ventral roots. This bursting pattern in the unlesioned, caudal thoracic-lumbar control preparations is similar to the activity recorded from ventral roots in isolated brainstem–spinal cord preparations (Kudo and Yamada, 1987; Smith and Feldman, 1987; Cazalets et al., 1992; Kiehn and Kjaerulff, 1996).

Activity after the lesion

After the lesion, the latency from the onset of tonic activity to discernible bursting was 5 ± 5 min (mean ± SD, $n = 45$ experiments). Although this latency statistically was significantly longer than before the lesion ($p < 0.001$, Wilcoxon paired-sample test), the difference was fairly small (mean difference 3 ± 3 min). The latency (11 ± 14 min) between discernible bursting and fully developed rhythmic activity was also significantly longer in lesioned preparations than before surgery, and this difference was more substantial (mean difference 8 ± 15 min, $p < 0.005$). Because rhythmic activity thus developed somewhat more slowly in the lesioned spinal cords, at least 2 hr were allowed to pass after surgery before the lesioned preparations were considered incapable of generating rhythmic activity in the used concentration (see Materials and Methods).

The localization of rhythm-generating networks as revealed by horizontal sections

Horizontal sections, extending the entire length of the preparation, were performed to evaluate the localization of rhythm-generating networks along the dorsoventral axis. The level of section varied between preparations ($n = 8$). An example is shown in Figure 2, *A* and *B*. The horizontal section was done close to the base of the dorsal horns and totally divided the spinal cord into a ventral half and a dorsal half (Fig. 2*A*; the section is marked with the number *1* in the *diagram* in Fig. 2*E*, *right*). The ability of the isolated ventral half to generate rhythmic bursting was well preserved postlesioning (Fig. 2*B*) compared with activity in the intact control preparation. Thus, left/right alternation and rostrocaudal alternation were still present after the lesion and, in this case, the modulation amplitude was only slightly reduced. It was not possible to assess whether any rhythmic activity was generated in the isolated dorsal half itself, because no locomotor-related potentials were observed in the dorsal roots in the newborn rat, not even in the intact cord, in contrast to the situation in other preparations (Baev, 1978; Dubuc et al., 1985; Ho and O'Donovan, 1993).

Normally coordinated rhythmic activity was also preserved after all other horizontal sections that did not pass below the level of the central canal. The most ventral of these sections was done at the anterior rim of the central canal (section marked with the number *2* in Fig. 2*E*, *right*). After this lesion, rhythmic activity was lost in the caudal recordings, but rhythmicity with left/right alternation persisted rostrally (not shown).

When the section was placed anterior to the central canal ($n = 3$; Fig. 2*C*, marked with the number *3* in Fig. 2*E*, *right*), only tonic activity was observed after 5-HT and NMDA in the isolated ventral fragment. Lesions anterior to the central canal may include the motoneuron pool, because the dorsal border of the lateral motoneuron columns can reach this level (Molander et al., 1984). Because the motoneurons are the output elements of the rhythm-generating network, it was necessary to assess whether rhythmic activity was lost after the lesion because the motoneurons had been extensively damaged. The ventral descending tracts from the rostral cut end of the preparation were therefore stimulated. A clear response was observed in all four ventral root recordings (Fig. 2*D*), showing that the motoneurons were able to respond to at least some synaptic input. Furthermore, although no phasic activity in 5-HT and NMDA was seen after the lesion, tonic activity did appear (Fig. 2*C*), demonstrating that the motoneurons were still able to respond to the neurochemicals directly or indirectly through synaptic input from activated in interneurons. In view of these observations, we conclude that the total loss of rhythmic activity after the extreme ventral horizontal lesions shown in Figure 2*C* most likely is attributable to a disconnection of the rhythm-generating network from the motoneurons (however, see Discussion).

The period was calculated for 10 consecutive cycles before and after horizontal sectioning (Fig. 2*E*, *left*). When the preparations with preserved rhythmicity were considered as a group, there was no significant mean period change after the lesion (paired *t* test; $n = 5$; $p > 0.2$).

The changes in relative modulation amplitude resulting from horizontal lesions are plotted in Figure 2*E* (*middle*). There was a significant reduction in the mean modulation amplitude in cases with preserved rhythmic activity ($p < 0.01$).

The main conclusion from the experiments involving horizontal lesions is that the networks contained in the ventral third of the spinal cord are sufficient to generate normally coordinated rhythmic activity, although with a reduced modulation amplitude.

Localization of rhythm-generating networks as revealed by sagittal sections

To assess the rhythmogenic capability of the lateralmost regions of the spinal cord, sagittal sections were done at varying distances from the midline. One such experiment is shown in Figure 3*A–C*. The section was done on the right side, approximately between the midline and the lateral edge of the preparation (Fig. 3*B*, section marked with the number *2* in 3*D*, *right*). The section left a small lateral fragment and a larger fragment consisting of the medial part of the right side and the entire left side of the cord (Fig. 3*B*). Rhythmic bursting could be induced in the larger fragment, whereas only unmodulated activity was observed in the smaller, lateral fragment (Fig. 3*A*).

The activity observed before and after sagittal sections is shown for all experiments in Figure 3*D* (small, lateral fragments; $n = 7$) and Figure 3*E* (large fragments; $n = 7$). The level is indicated separately for the smaller and larger fragments because it was impossible to avoid some tissue loss during the lesioning process.

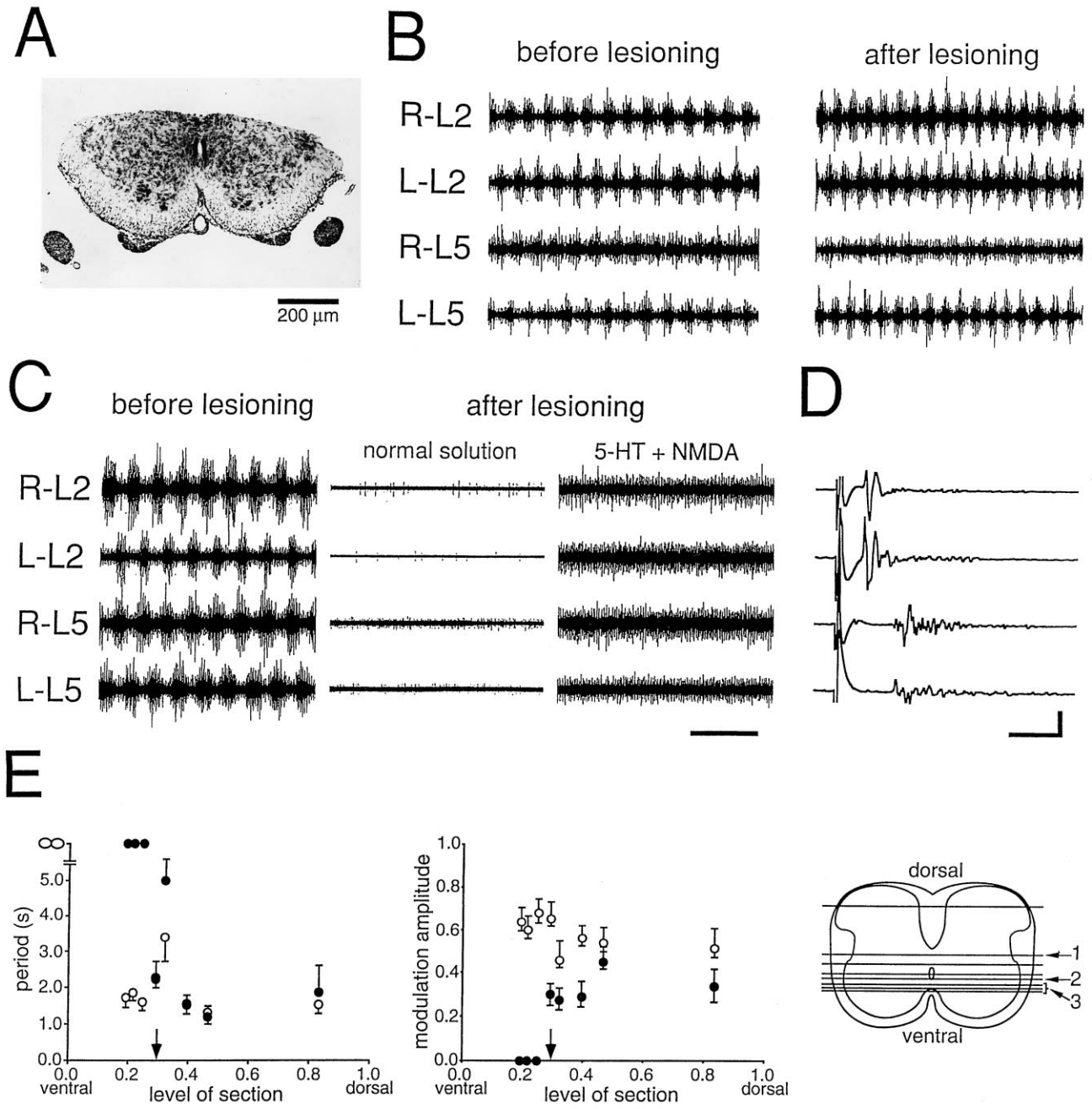

Figure 2. Activity in ventral fragments after horizontal sectioning. *A, B*, Rhythmic activity before (*B, left*) and after (*B, right*) a horizontal section removing the dorsal half of a Th12–L6 preparation. The remaining ventral half is shown on the micrograph in *A*. The section is indicated by the number *1* in the diagram in *E* (*right*). Rhythmic activity with left/right and rostrocaudal alternation persisted after the lesion with a slight reduction in modulation amplitude. Drug concentrations: 7.5 μM 5-HT, 7.5 μM NMDA. *C, D*, A different preparation (Th12–S1) with a more ventral lesion (indicated by the number *3* in *E, right*). The combination of drugs (20 μM 5-HT, 7.5 μM NMDA) that induced a clear rhythm before the lesion (*C, left*) only induced tonic activity after the lesion (*C, right*). *D*, It was still possible to elicit a ventral root response in all roots by stimulating the rostral end of the preparation, indicating that motoneurons were able to respond to synaptic input. *E*, *Left*, The period (mean and SD) against the level of section before (*open circles*) and after (*closed circles*) horizontal lesions for all preparations. The same set of 5-HT and NMDA concentrations was used before and after the lesion. The period was considered infinite when no rhythmic activity was observed. The level of section (shown directly on the *right*) is expressed as a fraction of the distance from the ventral to the dorsal border of the gray matter. The position of the central canal is indicated by an *arrow* above the *x*-axis. *E, Middle,* The relative modulation amplitude against the level of section. The *upward deflecting error bars* represent the SD of the peak amplitude, whereas *downward deflecting error bars* represent the trough amplitude SD. Both SDs were divided by the mean peak amplitude. *E, Right*, Schematic of all the lesions. The *numbers* are referred to in the text. Scale bars: 5 sec in *B* and *C*; 20 msec, 200 μV in *D*.

Regular, rhythmic activity was observed only in one small, lateral fragment resulting from the most medial section (marked with the number *1* in Fig. 3*D*, *right*). Bursts in the L2 and L5 recordings alternated (not shown), but the relative modulation amplitude was lower and the period considerably slower than before the lesion (Fig. 3*D*, *left* and *middle*). The width of the gray matter in the fragment was 63% of the width on the contralateral side. In all other cases, after more lateral sagittal sections, no rhythmic ac-

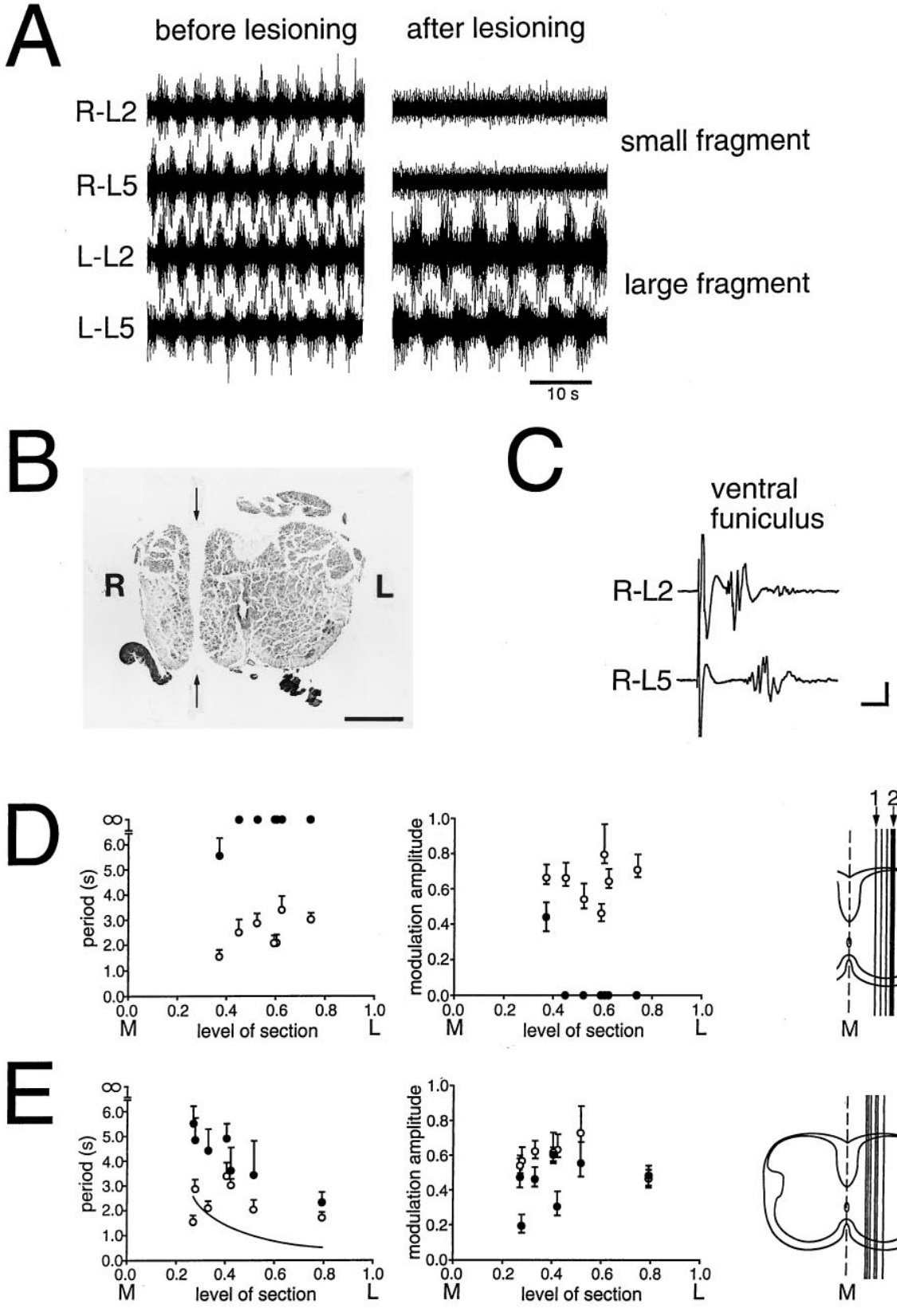

Figure 3. Activity in fragments left from sagittal sections. *A*, Before sagittal sectioning (*left*), 20 μM 5-HT and 7.5 μM NMDA induced a regular bursting pattern in an intact Th12–S1 preparation. After sectioning, the same drug concentration failed to induce rhythmic activity in the small fragment (*top two traces*, *right*; indicated by the number *2* in *D, right*), whereas it was preserved in the large fragment (*bottom traces*, *right*) of the cord, although with a longer period. *B*, Micrograph of a transverse histological section of the preparation in *A* showing the localization of the lesion (*arrows*). Scale bar, 200 μm. *C*, Ventral root responses to stimulation of the ventral funiculus on the rostral end of the small fragment. Scale bars: 10 msec, 100 μV. *D*, Summary of activity in all small fragments left from sagittal sections. Period (*left*) and modulation amplitude (*right*) before the lesion (*open circles*) are shown with the

tivity was observed in the lateral fragment when the same concentration of 5-HT/NMDA was used as before the lesion (Fig. 3*D*, *left*). In one experiment, the concentration of 5-HT/NMDA was increased compared with the control concentration (in which no activity was seen). This fragment measured 39% of the width of the gray matter, and a very slight modulation of the L2 ventral root activity was observed in the higher concentration.

The general absence of rhythmic activity in small, lateral fragments was hardly because of damage of motoneurons, because (1) in all cases, stimulating the descending tracts yielded clear responses in both the L2 and L5 ventral roots (illustrated in Fig. 3*C*) and (2) application of 5-HT/NMDA elicited discharges, although unmodulated, in the ventral root recordings.

In the larger fragments left from the parasagittal sections, rhythmic bursting with rostrocaudal alternation was observed in all cases. The lesion was followed by a progressively larger increase in the period length as the level of section approached the midline (Fig. 3*E*, *left*). Furthermore, the period increase was more dependent on the level of section in the medial than in the lateral region. Thus, the period increase versus the level of section was well fitted with a power function (linear regression after logarithmic transformation, $r = 0.80$, $p < 0.05$, curve in Fig. 3*E, left*). This might be taken as evidence for a predominantly medial localization of the rhythm-generating networks (see Discussion).

On average, there was a significant reduction in the relative modulation amplitude when compared with the same side before the lesion (Fig. 3*E*, *middle*; paired *t* test; $n = 7$; $p < 0.05$).

Based on these results, we conclude that crucial elements of the networks generating rhythmic activity are not very likely to reside in the lateralmost gray matter.

Pathways mediating left/right coordination are distributed along the cord

In recent experiments by Cazalets et al. (1995), it was concluded that the networks responsible for left/right alternation are restricted to the L1–L2 segments. This conclusion was based on experiments in which preparations were surgically split midsagitally caudal to L2. When transmitters were added to the superfusion medium at the L1–L2 level, left/right alternation was observed not only in L1–L2, but also in L3–L5. We have taken these experiments one step further by performing either rostral or caudal midsagittal sections and using circular statistics to analyze the coupling between the two sides. Our results suggest that left/right coordination is distributed along the entire rostrocaudal axis in the caudal thoracic-lumbar spinal cord.

Caudal midsagittal sections

Two Th12–L6 preparations had their L3–L6 segments split in the midline (*schematic* in Fig. 4*B2*, *lower right corner*). Rhythmic bursting before the lesion in one of these preparations is shown in Figure 4*A1*. Twenty-five consecutive phase values of the burst onsets in the left L2 ventral root were calculated with regard to the right L2 burst onsets. These phase values were plotted on a linear scale against cycle number to focus on their change over time. The phase values were relatively constant (Fig. 4*A2*, *top*). In addition, a circular plot was made of a random sample containing 25 phases from the whole episode of rhythmic activity (Fig. 4*A2*, *bottom*). As expected from an intact preparation, the mean phase value was close to 0.5, defining the coordination pattern as alternation.

Figure 4*B1* shows raw recordings obtained from the same preparation after caudal midsagittal splitting. After the lesion, an incidence of phase drift, i.e., a systematic time-dependent change in the phase value, was observed. (In Fig. 4*B1*, a tendency to show two bursts per cycle was seen in R–L2. Only the short-duration, high-amplitude bursts similar to those seen in control were considered in the analysis of phase relationships.) Early in the recordings, the onset of the R–L2 burst is leading the L–L2 bursts onset. A few cycles later, the R–L2 and L–L2 onsets are in phase, before L–L2 finally leads R–L2. This phase drift is better appreciated in Figure 4*B2* (*top*), where phases have been plotted against time. The phase drift is indicative of a weak coupling between burst activity on the two sides, and because phase drift was not observed in the unlesioned preparation (or in any other control), it was considered to result from the lesion. Weaker coupling after the lesion was also reflected in an increased dispersion of phase values around the mean (Fig. 4*B2*, *bottom*). The reduction in coupling strength postlesioning was statistically significant ($p < 0.001$).

Although the coupling strength was reduced after the lesion, significant coupling was preserved ($p < 0.001$). This conclusion is in agreement with the fact that the phase drift incidence was a solitary event covering approximately 25 cycles out of a total of 460 cycles. Also, during most of the episode, the phase values on average stayed fairly close to 0.5, as before the lesion (compare Fig. 4*A2,B2*, *bottom*).

In another preparation, there was no significant change in the coupling strength after a caudal midsagittal section ($p > 0.2$). However, in this case, the concentration of rhythm-inducing neurochemicals had to be increased compared with control to reinduce rhythmic bursting.

These experiments corroborate the observation by Cazalets et al. (1995) that the rostral segments contain crossing connections sufficient to mediate left/right alternation. However, coupling was also observed to be weaker after the lesion, suggesting that the pathways coordinating bilateral activity may extend to caudal segments. This notion was confirmed by the experiments described in the next section.

Rostral midsagittal sections

If the pathways crossing rostrally are not only sufficient (as just shown), but also necessary to mediate left/right alternation both at the L2 and L5 level, then a midsagittal section involving this rostral region should totally abolish the alternation. This lesion was done in three experiments, one of which is shown in Figure 5.

←

corresponding measurements on the same side after the lesion (*closed circles*). In all cases, the same concentrations of 5-HT and NMDA were used before and after the lesions. The level of section is indicated as a fraction of the distance from the midline (*M*, *below abscissa*) to the lateral border of the gray matter (*L*). The schematic on the *right* shows the position of the medial border of the lateral fragment in the transverse plane. *E*, Summary of activity in all large fragments left from sagittal sections. Graphs as in *D*. The schematic on the *right* shows the position of the lateral border of the large fragment in the transverse plane. Note that the level of the cut surfaces differed in the smaller and larger fragments even when they were derived from the same preparation, as was generally the case (see text). Rhythmic activity was present in all large fragments, but it was only observed after the most medial section in the small fragments (indicated by the number *1* in *D*, *right*). The period increase as a function of the section level in the large fragment was fitted with a power function (*curve* in *E, left*; data points omitted for clarity).

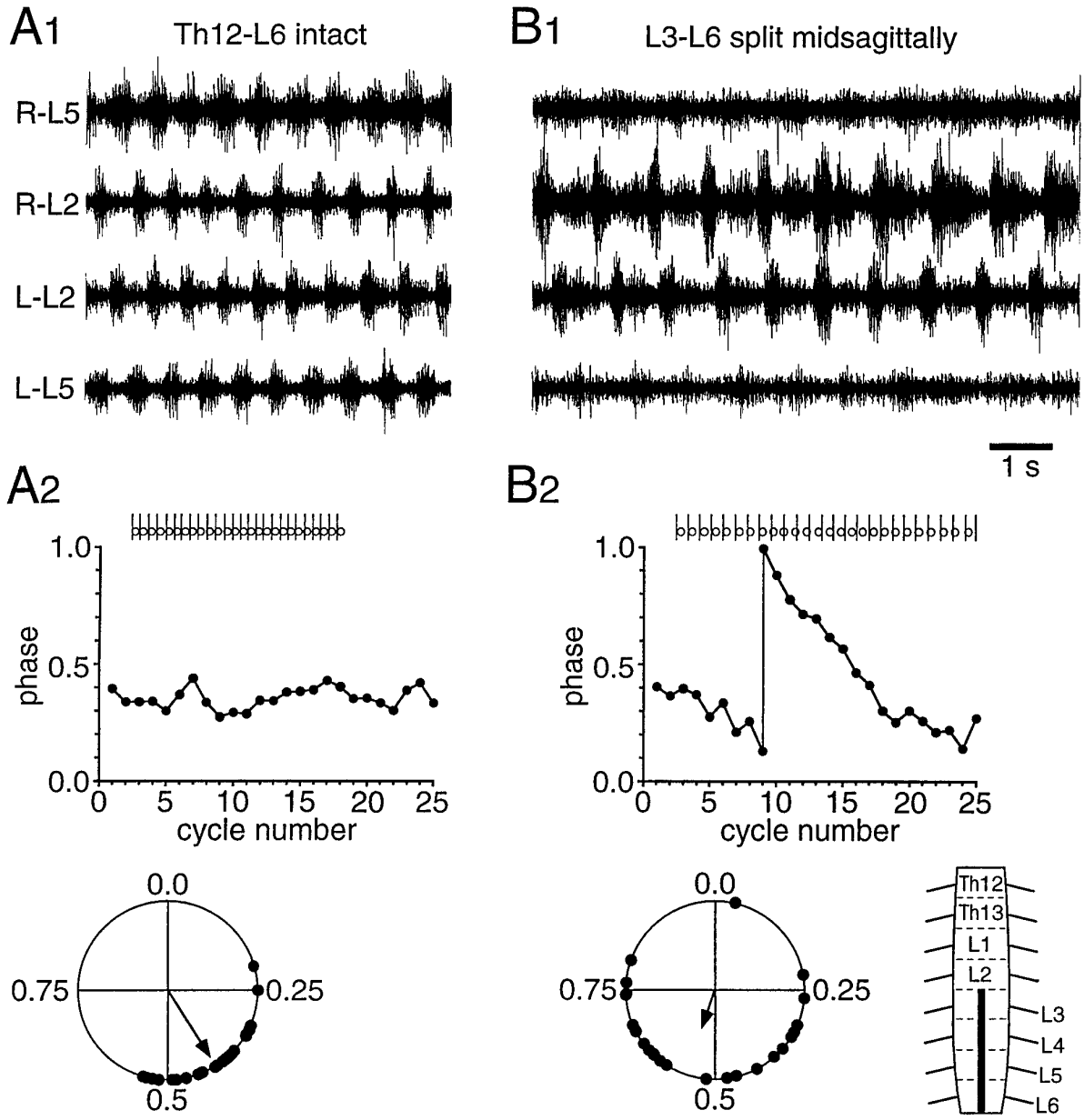

Figure 4. Left/right coupling mediated through the Th12–L2 segments. *A1*, Rhythmic activity in an intact Th12–L6 preparation. *A2*, Linear plot (*top*) of the phase values of 25 consecutive L-L2 onsets calculated with respect to R-L2 onsets. The basis of this calculation appears from the *raster plot* above the graph showing the relative timing of R–L2 onsets (*sticks*) and L-L2 onsets (*open circles*). A *circular plot* of 25 phase values picked at random from the whole episode of rhythmicity is seen at the *bottom*. The direction and length of the *vector* in the *circular plot* indicate the mean phase and the concentration of phase values around the mean phase, respectively. *B1*, An episode of phase drift in the same preparation after a midsagittal section of the L3–L6 segments illustrated in the schematic in the *lower right corner* of *B2*. *B2,* The episode of phase drift plotted on a linear scale (*top*). The *circular plot* (*bottom*), which is based on 25 phase values picked at random, shows the highly reduced concentration of phase values around the mean phase, indicating looser coupling after the lesion. Only the short, high-amplitude bursts similar to those seen before the lesion are considered in the phase analysis. Drug concentrations: 5.5 μM 5-HT, 5.5 μM NMDA.

Rhythmic activity with left/right alternation was first induced in an intact preparation (Fig. 5*A*). When rhythmic activity was induced a second time, but after the segments Th12–L2 had been midsagittally sectioned (see *schematic* in Fig. 5*B1*, *right*), the phase values centered around a mean of 0.6 (Fig. 5*B2*, *right*), indicating that the bursts in R–L2 and L–L2 still generally alternated. This coupling was significant ($p < 0.005$).

Although coupling was thus preserved after the rostral midline hemisection, the concentration of phase values was much reduced when compared with control ($p < 0.001$). This indicated that the coupling was indeed weakened. In accordance, early in the bursting episode one side often showed bursting with a constant period, whereas bursting on the opposite side was irregular (Fig. 5*B1*, *left* and *middle*). Later, phase-drift episodes occurred (Fig. 5*B2*, *left* and *middle*). Neither of these phenomena indicating looser coupling was observed before the lesion, where bursting was regular with constant alternation (Fig. 5*A*).

The observations above were done using the same 5-HT/

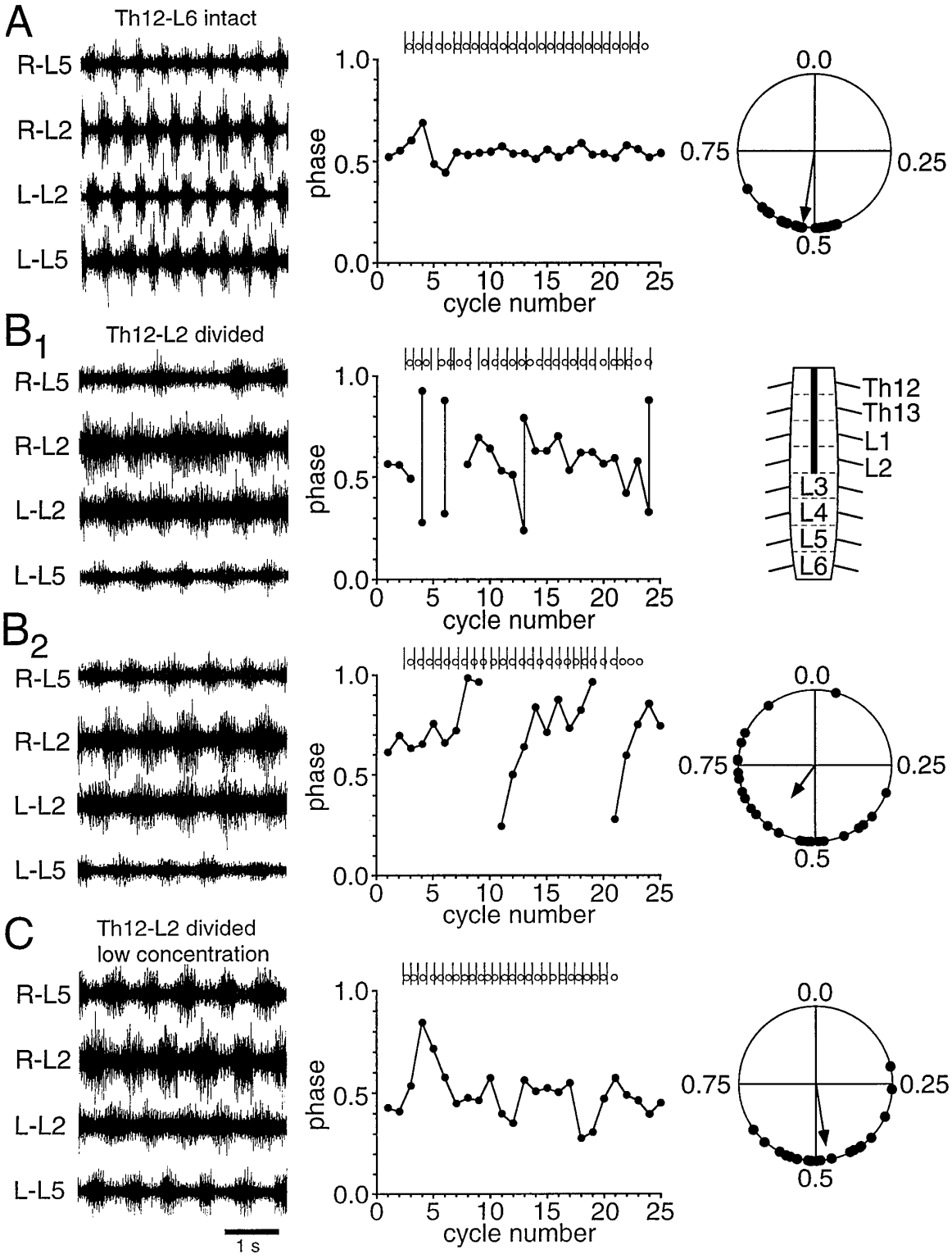

Figure 5. Left/right coupling mediated through the L3–L6 segments. *A*, Rhythmic activity (*left*; induced by 6 μM 5-HT and 6 μM NMDA) before the lesion in a Th12–L6 preparation, shown together with a *linear plot* of 25 consecutive phase values (*middle*) and a *circular plot* of 25 random cycles covering the whole episode of rhythmicity (*right*). *B1, B2*, Rhythmic activity (*B1, B2, left*), linear (*B1, B2, middle*) and circular (*B2, right*) phase plots in the same preparation after a hemisection of the Th12–L2 segments (indicated in the *schematic*, *B1*, *right*). During the first part of the recording, sudden changes in period, not affecting contralateral bursting, appeared on both sides. As a result, two bursts could occur on one side that were not separated by a contralateral burst onset (*B1*, *left* and *middle*). Later, the period became more constant, but phase drift now occurred (*B2*, *left* and *middle*). These features indicating looser coupling were not observed before the lesion. Coupling was still significant, although the concentration of phases around the mean was reduced (compare *A*, *right* and *B2*, *right*). *C*, Rhythmic activity induced by lower drug concentrations (5.5 μM 5-HT, 5.5 μM NMDA) after the lesion in the same preparation as in *A*, *B1*, and *B2*. The concentration of phase values around the mean again increased (*C*, *middle* and *right*), and the coupling was not significantly lower than during bursting in the higher concentration before the lesion (compare *A*, *right* and *C*, *right*).

NMDA concentration pre- and postlesioning. Interestingly, when rhythmic bursting was induced a second time after the lesion with a slightly lower 5-HT/NMDA concentration, coupling was potentiated (Fig. 5*C*; significant coupling, $p < 0.0000001$). Now, no phase drift was observed, and the dispersion of phase values decreased, again approaching the control level (compare Fig. 5*A*, *right* with Fig. 5*C*, *right*). Also, the mean phase 0.48 was close to the value of 0.50 indicating strict alternation, as before the lesion.

In a second preparation with Th12–L2 split midsagittally, significant coupling was also preserved when the same 5-HT/NMDA concentration as in control was used ($p < 0.0025$). However, an *increase* in 5-HT and NMDA concentrations weakened the coupling and made it insignificant ($p > 0.02$). Thus, the concentrations of rhythm-inducing drugs in these experiments were inversely correlated to the coupling strength. However, more experiments are needed to determine the precise relationship between drug concentration and left/right coupling.

In a third experiment involving rostral splitting, bursting was strongly irregular after the lesion, excluding a meaningful coupling analysis.

Together, these experiments suggest that the left/right coordinating systems are distributed along the cord (for alternation in an isolated L4–L6 preparation, see Fig. 9*C*). The rostral coupling seems, however, to be more dominant than the caudal coupling.

Left/right coordination pathways are localized in the ventral commissure

Although the experiments described above show that the fibers mediating left/right coordination are distributed along the cord, they do not localize the pathways in the transverse plane. However, midline structures ventral to the central canal are sufficient to mediate the left/right alternation. This follows from the fact that left/right alternation may be preserved in a ventral fragment left from a horizontal section in the plane of the central canal (see above: *Localization of rhythm-generating networks as revealed by horizontal sections*). To investigate whether the ventral pathways are also necessary to coordinate bilateral rhythmicity, ventral lesions were done along the whole rostrocaudal extent of caudal thoracic-lumbar spinal cord preparations ($n = 5$). In one experiment, the lesion included the ventromedial aspect of both ventral horns, removing the overlying white matter and a minor part of lamina VIII. The ventral commissure was kept intact. Alternation was not abolished by this lesion (not shown). In contrast, as illustrated in Figure 6 by the raw recordings (Fig. 6*C*, compare Fig. 6*A*) and the circular phase plots (Fig. 6*D*, compare Fig. 6*B*), left/right alternation was completely eliminated when the lesion reached the anterior rim of the central canal (Fig. 6*E,F*; $n = 3$). In a fifth preparation in which the ventral commissure was only partly severed, there was a substantial reduction in the coupling between the two sides compared with control. Based on these results and the experiments with horizontal lesions, we conclude that left/right alternation seems to be mediated exclusively by fibers crossing in the ventral commissure.

Pathways mediating rostrocaudal coordination are distributed in the transverse plane

To further characterize the pathways coordinating locomotor movements, experiments were done to localize the pathways that mediate the alternation between bursts in L2 and ipsilateral L5. Combined ventral root and electromyographic (EMG) recordings have shown that this pattern is equivalent to flexor/extensor alternation, with L2 bursts occurring concomitantly with bursts in ipsilateral flexor muscles, and L5 bursts in phase with extensors (Kiehn and Kjaerulff, 1996).

Effect of creating a lateral bridge

A lateral bridge was created in five preparations. In two experiments with identical results, the lesion consisted of a partial excision of the L3 segment. An example is shown in Figure 7. A bridge consisting mainly of the lateral funiculus connected the rostral and caudal regions after the lesion (Fig. 7*A*). When rhythmic activity was reinduced, bursts alternated between R-L2 and R-L5 (Fig. 7*C*), as before the lesion (Fig. 7*B*).

Although the creation of a lateral bridge did not affect alternation ipsilateral to the bridge, it did change the bursting activity. Thus, the relative modulation amplitude was somewhat reduced on the side ipsilateral to the bridge, and rhythmic bursting was abolished in the contralateral L5 ventral root. In contrast, the bursts in R–L2 and L–L2 showed no reduction in the modulation amplitude (Fig. 7*C*). The effects on the modulation amplitude are discussed further in a later section.

Results qualitatively similar to those shown in Figure 7 were obtained in two other preparations (one of which was a large fragment from a sagittal section), where either the L3 or L4 segment was partially removed. In the remaining preparations, the lateral bridge had an even larger rostrocaudal extent, covering both L3 and L4. In this case, it was not possible to evaluate the rostrocaudal coordination because rhythmic activity was abolished caudally to the bridge both ipsilaterally and contralaterally.

In conclusion, the region roughly corresponding to the lateral funiculus contains sufficient connections to mediate the burst alternation in the L2 and L5 ventral roots.

Effect of creating a median bridge

Figure 8 illustrates the ability of median pathways to mediate rostrocaudal alternation. Rhythmic activity was induced (Fig. 8*C*) in a preparation in which the lateral funiculus and 35% of the lateralmost gray matter had been removed bilaterally from the L3 segment (Fig. 8*A*, *top schematic*; activity before the lesion in Fig. 8*B*). After this lesion, rhythmic bursting persisted in all four recordings, although with a reduced modulation amplitude, especially in the caudal recordings (Fig. 8*C*). Importantly, rostrocaudal alternation was preserved, which means that coordinating pathways not only exist in the lateral funiculus, but also occupy the median aspect of the cord (Fig. 8*C*). Similar results were obtained in three other experiments in which the width of the bridge measured as the percentage of the total width of the gray matter ranged from 47 to 100% (with 100% implying the selective removal of white matter).

At least part of the median pathways mediating rostrocaudal alternation in median bridge preparations were expected to reside within the ventral funiculus. This was tested directly in the experiment shown in Figure 8. When the ventral funiculus was totally isolated in the transverse plane, still at the L3 level (Fig. 8*A*, *lower schematic* and *micrographs*), the rostrocaudal alternation persisted (Fig. 8*D*). Therefore, pathways mediating rostrocaudal alternation must exist in the ventral funiculus.

Effect of midsagittal and ventral lesions on rostrocaudal alternation

As shown in Figures 4, 5, and 6, rostral and caudal midsagittal lesions and ventral lesions had no obvious effects on rostrocaudal alternation, suggesting that these pathways do not participate in generating the alternation between L2 and L5.

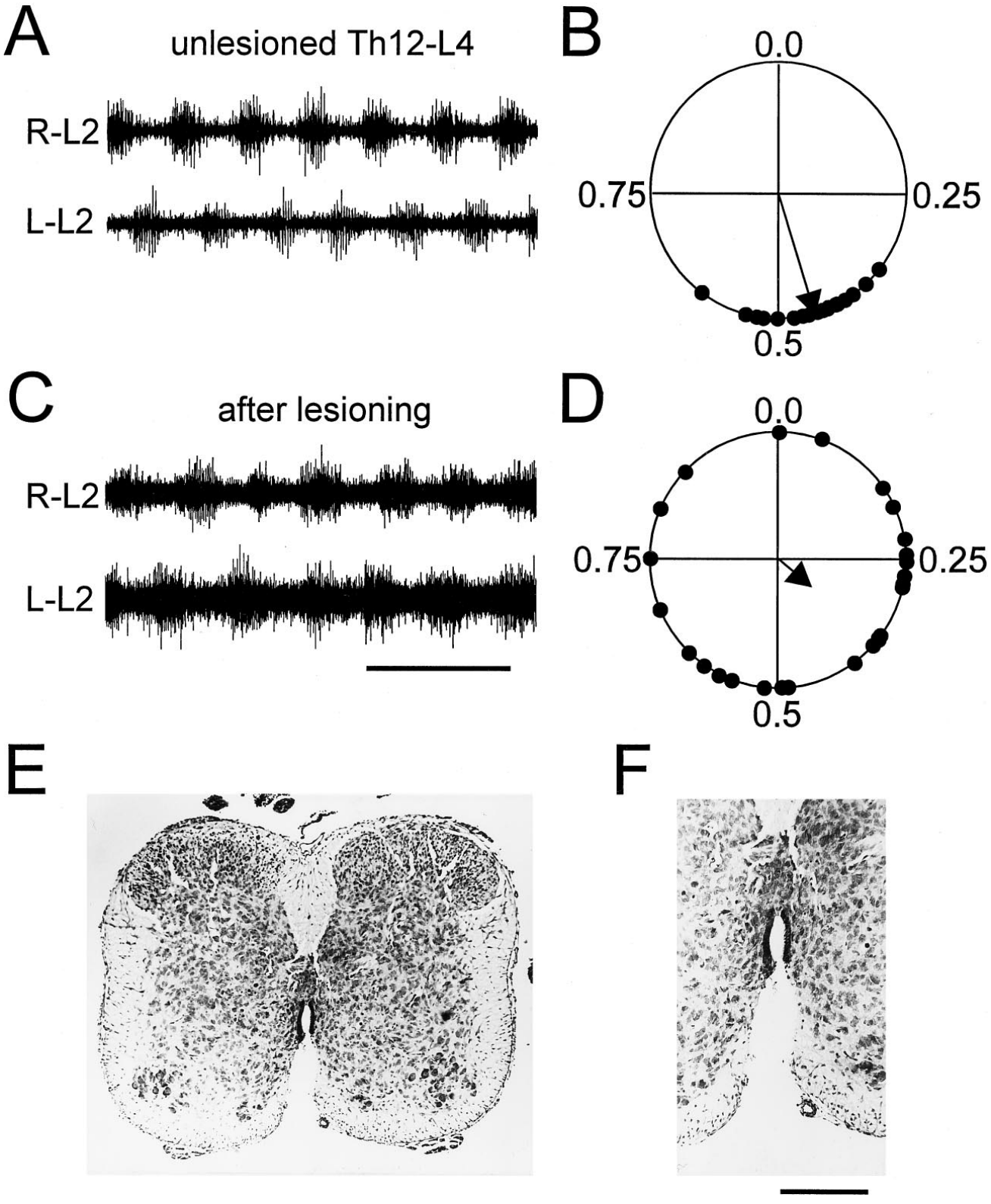

Figure 6. Left/right alternation depends on an intact ventral commissure. *A, B*, Raw recordings (*A*) and circular phase plot (*B*) showing left/right alternation in an intact Th12–L4 preparation. *C*, *D*, After cutting the ventral commissure along the whole rostrocaudal extent of the cord, coupling became insignificant ($p > 0.1$). Another observation was a slowing of the period after surgery (time calibration: *A*, 2.5 sec; *C*, 10 sec). A period increase was seen in all preparations after ventral lesions uncoupling the two sides. *E, F*, Photomicrographs showing the lesion in overview (*E*) and in higher magnification (*F*). Drug concentrations: 15 μM 5-HT, 7.5 μM NMDA. Scale bar: 300 μm in *E*, 500 μm in *F*.

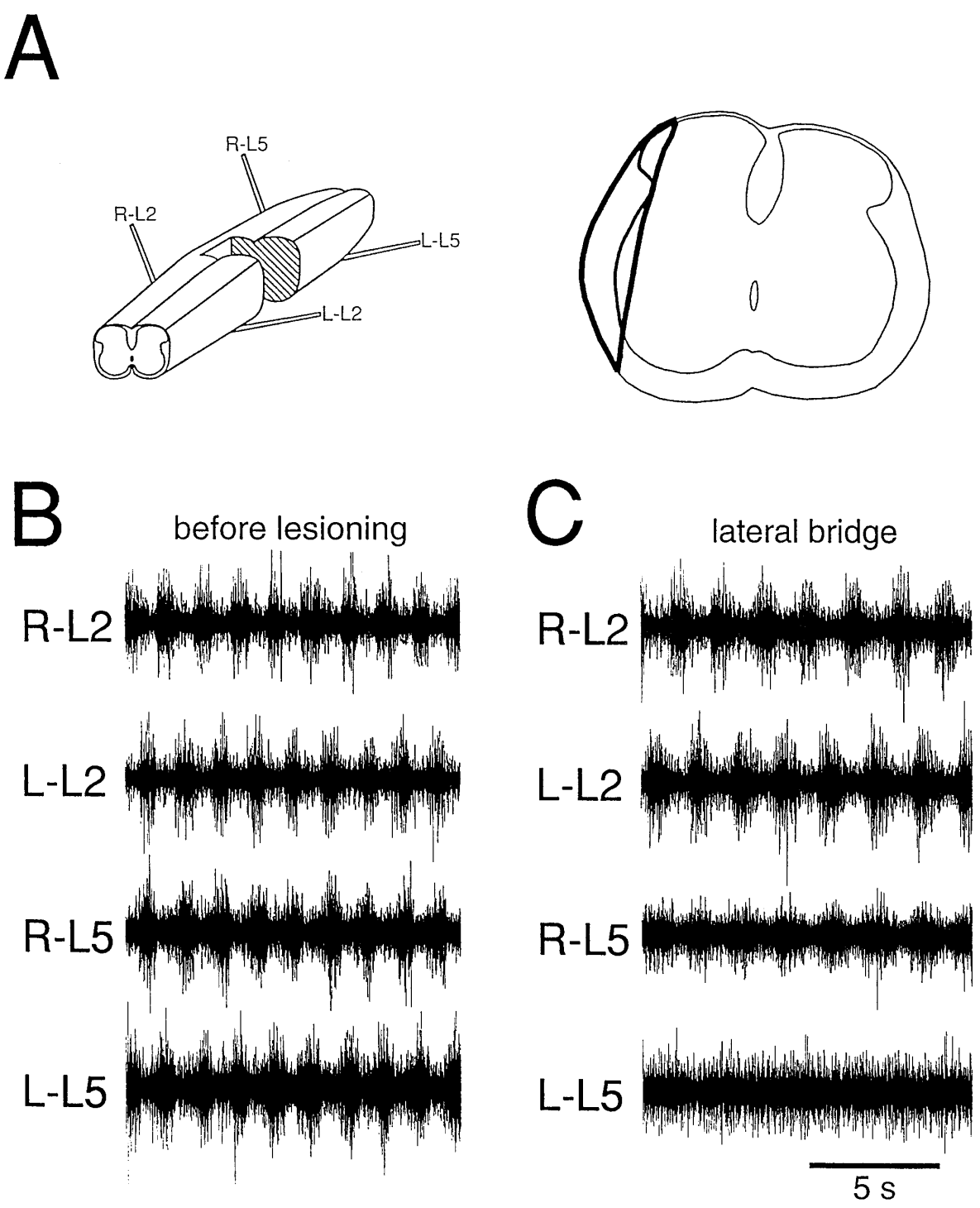

Figure 7. Rostrocaudal coordination mediated by the lateral funiculus. *A*, A lateral bridge (*left schematic*) was created at the L3 level. The *right schematic* shows the transverse extent of the bridge (*thick line*). Rostrocaudal alternation, observed before the lesion (*B*), persisted after creation of the bridge (*C*). On the ipsilateral side, caudal rhythmic activity showed a reduced modulation amplitude, but only tonic activity was observed contralaterally to the bridge. Rostral bursting was not severely affected by the lesion. Drug concentrations: 7.5 μM 5-HT, 7.5 μM NMDA. Th12–S1 preparation.

The ability to generate rhythmic activity in rostral and caudal segments

Lateral/median bridge experiments

In this section, the changes in modulation amplitude seen in the lateral and median bridge preparations are discussed more extensively. As already shown, there was a differential effect on the modulation amplitude in the L2 and L5 ventral roots after partial removal of the midlumbar segments (Figs. 7, 8). These changes were evaluated statistically. At the L2 level, there was a small and insignificant reduction in the relative modulation amplitude in the (pooled) lateral and median bridge preparations compared with intact control preparations (mean reduction 0.05; $n = 7$; paired t test). In contrast, in lateral bridge preparations no rhythmic activity in the L5 root contralateral to the connection was visible

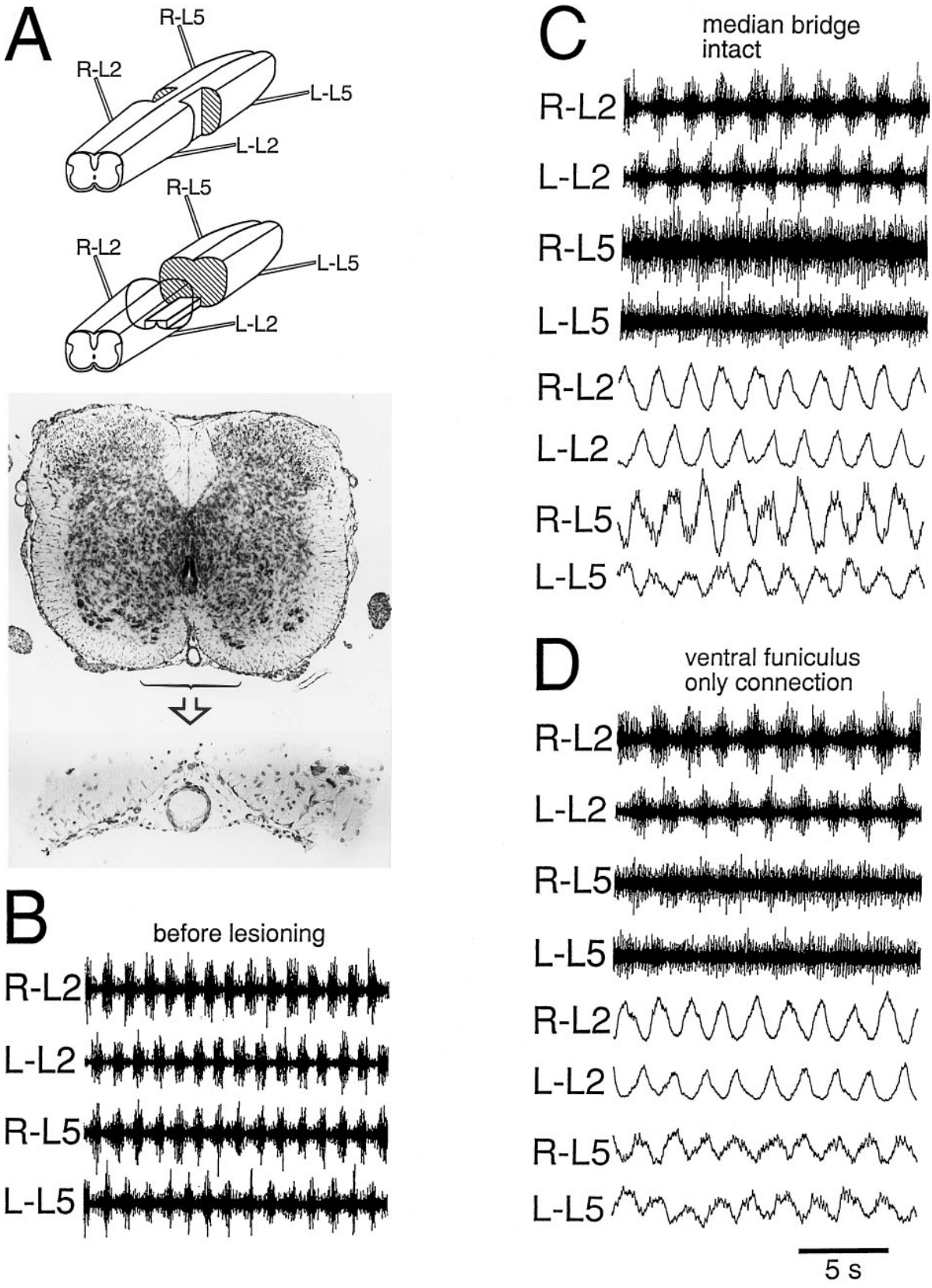

Figure 8. Rostrocaudal coordination mediated by median pathways or the isolated ventral funiculus alone. After the creation of a median bridge at the L3 level (*top schematic* in *A*), bilateral rostrocaudal and left/right alternations were preserved (*C*). The activity before the lesion is illustrated in *B*. After removal of the majority of the bridge leaving only the ventral funiculus to connect the rostral and the caudal region of the preparation (*middle schematic* in *A*), bilateral rostrocaudal and left/right alternations were still preserved (*D*). A transverse histological section of the bridge (the ventral commissure) is shown in *A* (*bottom*), together with a section of the intact cord just outside the lesioned segment. Th12–S1 preparation. Drug concentrations: 7.5 μM 5-HT, 7.5 μM NMDA.

Table 1. Summary of the rhythm-generating potential along the cord

Rostral	Caudal	Average no. segments	Preparations with rhythmic activity	Relative modulation amplitude	Period length	Period coefficient of variation
Th11–Th12	Th13	2.7 ($n = 3$)	100%	0.96 (0.54–1.30)	1.01 (0.94–1.08)	3.99 (1.32–6.12)
Th12	L1–L2	3.3 ($n = 7$)	100%	0.84 (0.63–1.22)	1.16 (0.75–1.86)	2.13 (0.50–3.51)
Th13	L1–L2	2.3 ($n = 3$)	100%	0.59 (0.42–0.70)	1.30 (0.75–1.92)	4.29 (1.07–8.89)
L1	L3–L6	5.0 ($n = 3$)	100%	0.75 (0.62–1.00)	1.17 (1.03–1.38)	3.88 (2.61–6.22)
L2	L4–L6	4.5 ($n = 3$)	67%	0.76 (0.72–0.78)	1.38 (1.17–1.59)	2.53 (2.25–2.82)
L3	L6–S1	4.4 ($n = 5$)	80%	0.66 (0.57–0.70)	2.95 (1.52–5.53)	5.33 (2.16–9.76)
L4	L5–L6	2.8 ($n = 6$)	33%	0.61 (0.38–0.83)	2.71 (1.46–3.97)	4.27 (3.92–4.63)

The first two vertical columns identify the rostral and caudal borders of surgically divided short preparations. The average number of segments and number (n) of preparations used are given in the third vertical column; the fourth column shows the percentage of rhythmically active preparations within each group. The relative modulation amplitude, period length, and the period coefficient of variation were divided by the corresponding measurements before the lesion. The mean, followed by the range (in parentheses), is presented for this ratio.

(Fig. 7*C*). Furthermore, in the L5 roots ipsilateral to a lateral bridge (Fig. 7*C*) and the L5 roots caudal to a median bridge (Fig. 8*C*), there was a substantial reduction in the relative modulation amplitude (mean reduction 0.20; $n = 7$; $p < 0.01$; paired t test).

A natural interpretation of these results is that rhythmic activity recorded in the L5 roots depends on the presence of rostral rhythmic activity, i.e., the L3 segment or the more rostral segments directly or indirectly drives the activity seen in L5 before the lesion. However, this conclusion needs to be modified in light of the results presented in the next section.

Short preparations

Preparations were split into shorter pieces consisting of 2–6 segments, and their ability to generate rhythmic activity was then correlated with their origin on the rostrocaudal axis. Experiments of this kind are shown in Figure 9*A–C*.

In Figure 9*A–A2b*, rhythmic activity was induced in a Th12–L6 preparation (Fig. 9*A*). After wash, the preparation was divided into a rostral piece (Th12–L1) and a caudal piece (L2–L6). Regular bursting with left/right alternation could be induced in both the rostral (Fig. 9*A1a*) and the caudal preparation (Fig. 9*A1b*). Whereas the relative modulation amplitude was similar for the two preparations, the period was shorter in the Th12–L1 than in the L2–L6 preparation. The rostralmost segment was then excised from both the rostral and the caudal preparation. This did not notably affect rhythmic activity in the rostral preparation, now consisting of only two segments (Th13–L1; Fig. 9*A2a*). In contrast, in the caudal preparation with four segments, bursting became more irregular after the reduction and showed a lower modulation amplitude (L3–L6; Fig. 9*A2b*). As a result of these changes, the bursts in the rostral preparation not only continued having a shorter period, but, in addition, the period was more constant and the modulation amplitude higher than in the caudal oligosegment.

Rostrally generated rhythmic activity thus seems to dominate qualitatively. However, the ability to generate rhythmic activity is evidently not reserved to the rostral segments. Two examples of caudally generated rhythm are illustrated in Figure 9, *B* and *C*. Figure 9*B* shows regular bursting in a preparation consisting of the caudal two-thirds of L3 plus the intact L4–L6 segments, whereas Figure 9*C* depicts left/right alternating rhythmicity in an L4–L6 preparation.

The results from all experiments with short preparations are summarized in Table 1, in which the number of experiments is given and the occurrence and quality of rhythmic activity can be compared with the rostrocaudal origin of the preparations. Three main conclusions may be drawn from this table. First, the ability to generate rhythmic activity is distributed to all lumbar segments. These results are in contrast to split-bath experiments, in which only irregular activity was found in preparations with L2 as the most rostral segment exposed to rhythm-inducing neurochemicals, and only tonic activity occurred with L3 as the rostralmost segment (Cazalets et al., 1995) (see Discussion). Second, the relative modulation amplitude was lower, and the period mean and coefficient of variation were higher in the caudal lumbar segments (below L3) compared with the rostral lumbar segments. This indicates that, although the basic alternating pattern can be generated caudally, there appears to be a rostrocaudal gradient in the ability to generate rhythmic activity, as also reflected in the fact that only tonic activity was observed in ~65% of the L4–L5/L6 preparations. Third, rhythmic activity was found in isolated T11–Th12 / Th13 segments ($n = 3$). In one of these preparations in which recordings were performed on both sides of the cord, left/right alternation was observed. This left/right alternation was similar to that observed when the thoracic cord was connected to the lumbar cord. Therefore, despite their more distant anatomical location from the motoneurons innervating the muscles of the hindlimb, rhythm-generating networks in the caudal thoracic domain may at present be considered just as important for locomotor-related activity as the lumbar domain.

DISCUSSION

In this study, mechanical lesions were used to localize the neuronal networks controlling locomotion in the mammalian spinal cord. Our data suggest that the most important areas for rhythmogenesis are localized in the ventromedial aspect of the caudal thoracic and rostral lumbar segments. The rhythm-generating ability and the coordinating pathways are distributed both in the transverse plane and along the long axis of the cord. The fibers involved in left/right alternation appear to cross only in the ventral commissure, which is a notable exception to the generally diffuse wiring of the network. The relationship of our findings with findings obtained in previous studies of the organization of the spinal locomotor CPGs in the neonatal rat and other vertebrates is discussed below.

Localization of rhythm-generating networks in the transverse plane

In chick embryos, the ability to generate rhythmicity has also been shown to exist ventral to the central canal (Ho and O'Donovan, 1993). This indicates that in vertebrates in general, the most important elements of the CPG reside in the ventralmost regions of the spinal cord. Curiously, in the chick embryos rhythmicity

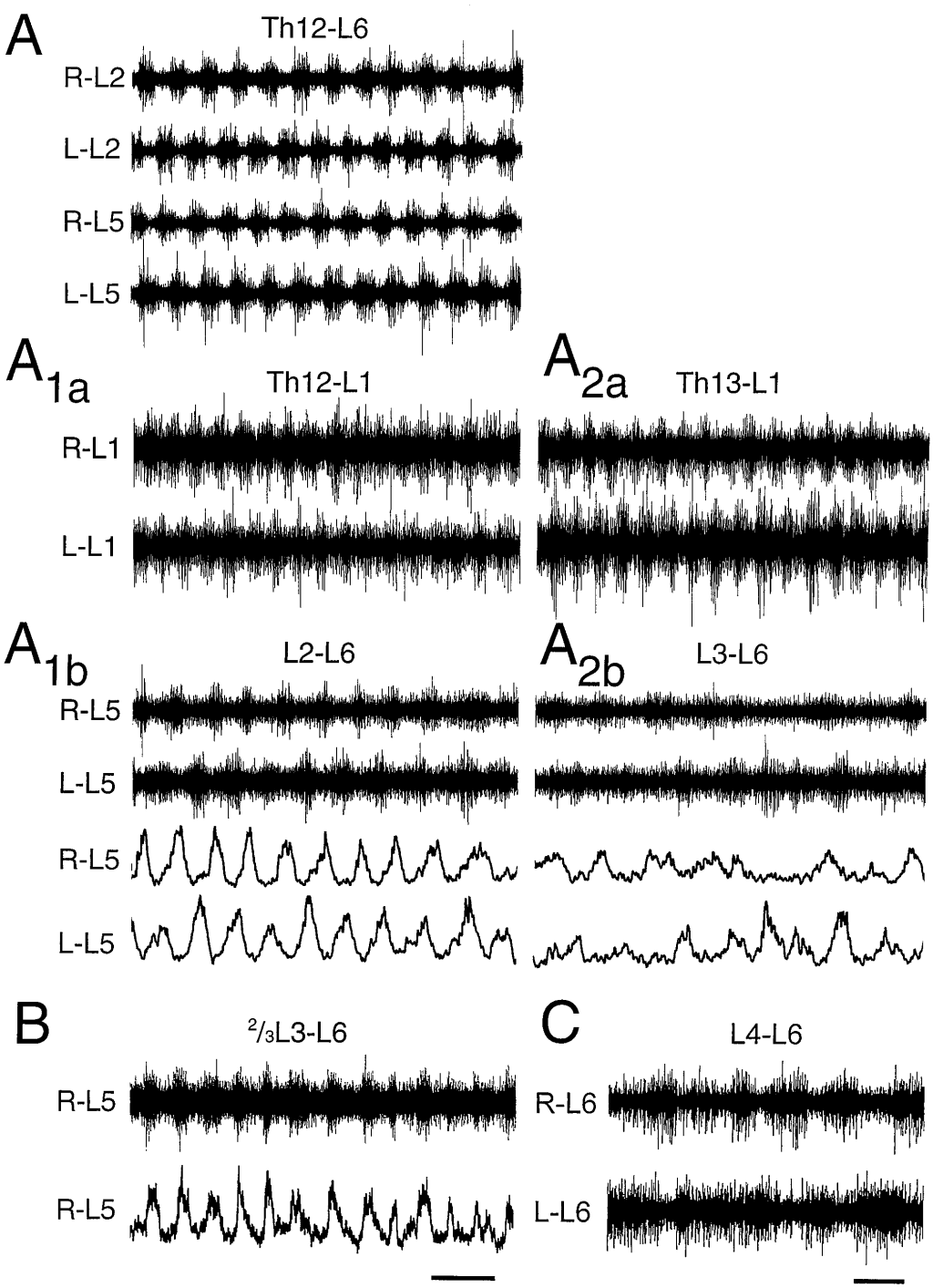

Figure 9. Rhythmic activity in spinal cord pieces consisting of few segments. *A*, Rhythmic activity in a Th12–L6 preparation. After dividing the T12–L6 preparation into two shorter pieces, a rostral part consisting of the Th12–L1 segments (*A1a*) and a caudal part consisting of the L2–L6 segments (*1A1b*), rhythmic activity could still be induced in both preparations. The period was shorter in the rostral preparation and, in this experiment, also shorter than during activity before the division (*A*). After further reduction of the two preparations by removing Th12 from the rostral preparation (*A2a*) and L2 from the caudal preparation (*A2b*), rhythm could still be induced in both preparations. The relative modulation amplitude was now higher in the rostral than in the caudal preparation. Drug concentrations: 7.5 μM 5-HT, 7.5 μM NMDA. *B*, Regular bursting in a caudal preparation consisting of two-thirds of the L3 segment and the intact L4–L6 segments. *C*, Data from an L4–L6 preparation showing rhythmic alternation in the L6 ventral roots. Drug concentrations: 9 μM 5-HT, 6 μM NMDA (*B*); 4.5 μM 5-HT, 4.5 μM NMDA (*C*). Scale bars: 5 sec in *A–A2b*, 10 sec in *B*; 5 sec in *C*. Data in *A–A2b*, *B*, and *C* are from three different animals.

could be elicited even after severe dorsal lesions leaving only 10% of the full ventral-to-dorsal extent of the gray matter. In contrast, in the newborn rat rhythmicity was not observed in ventral fragments measuring <25% of the ventral-to-dorsal extent. It is likely that networks in the adjacent more dorsal areas also contribute to rhythmogenesis. Thus, our previous sulforhodamine experiments (Kjaerulff et al., 1994) demonstrated substantial labeling in the ventromedial areas as well as more dorsal to the central canal.

Isolated lateral fragments of the spinal cord showed very weak or no rhythmicity, and rhythm-generating centers are therefore more likely to accumulate medially than laterally. Further experiments are needed to clarify whether the lateral rhythmogenic potential can be released consistently (e.g., by varying the transmitter concentration). It should be noted here that rhythmically active interneurons have been recorded during transmitter-induced locomotion both ventrolaterally (MacLean et al., 1995) and in the medial intermediate zone and close to the central canal (Kiehn et al., 1995, 1996). The role of these cells in the rhythm-generation itself has, however, not been determined.

Elimination of the locomotor rhythm after lesioning might result from mechanical separation of motoneurons or relay centers from neurons that generate the activity, or from physical damage to motoneuron dendrites that receive inputs from CPG elements. Our study cannot distinguish between these possibilities. It is therefore possible that the CPG resides laterally and projects to medially localized relay centers that in turn project to motoneurons. Alternatively, medially extending motoneuron dendrites that were cut away by the medial lesion receive synaptic input from a laterally located CPG. In both cases, it would imply that the rhythm-generating network is found within or close to the motoneuron pools, because rhythmic activity was preserved after horizontal sections removing the areas dorsal to the motor columns.

The reduction in modulation amplitude seen after both horizontal and sagittal sections may suggest that the drive from the CPG onto the motoneuron pools decreased. This could be attributable to a decrease in the activity of the excitatory CPG elements or the fact that motoneurons received less drive because of damage of distal dendrites. Alternatively, the reciprocal inhibition weakened, causing a decrease in the contrast between the motoneuronal excitatory and inhibitory phases. This would not affect the rhythm-generating ability because the rhythm can continue in the absence of inhibition (Cowley and Schmidt, 1995). Presently, we are unable to distinguish between these possibilities.

There was a substantial increase in locomotor period after medial sagittal sections and after lesioning the ventral commissure, whereas no significant change in the period was observed after horizontal sectioning. Such an increase in locomotor period in the neonatal cord has also been observed after a complete midsagittal section (Kudo and Yamada, 1987) and after blocking reciprocal inhibition with strychnine (Cowley and Schmidt, 1995). This suggests that the two sides of the cord may have to work together to generate a high-frequency rhythm and that part of the frequency control is dependent on inhibitory connections. The fact that the most lateral sagittal lesions only caused relatively minor changes in the period compared with medial lesions suggests that the lateral cord does not contain CPG elements of crucial importance for maintaining the high-frequency rhythm.

A final issue is the frequently observed increased delay in the appearance of fully developed rhythmic activity after lesioning. Possible explanations for this increased delay include the following: (1) mechanical depression of synaptic activity in the remaining tissue; (2) removal of tissue that has an excitatory influence on rhythm-generating areas; and (3) that previously silent synapses (Durand et al., 1996) were slowly recruited after the lesion eliminated synapses originally responsible for rhythm and pattern generation. At this point, it is impossible to distinguish between these ideas. However, the first two possibilities should not change the conclusions concerning the localization of the CPG stated previously. Regarding the third possibility, it is clear that a high degree of plasticity in the locomotor-related networks would complicate the interpretation of lesion or other isolation studies. It is possible that recruitment of silent synapses contributed to the observed improvement over time of the rhythmic activity in some lesioned preparations, i.e., that a learning process took place. It appears, however, that to recruit the appropriate silent synapses, rhythmic activity with the normal spatiotemporal pattern (which was always observed after the lesion when rhythm was preserved) must have been generated initially by a locomotor network functioning before any plastic changes occurred, because recruitment of silent synapses is activity-dependent and -specific (Durand et al., 1996).

Figure 10 summarizes the localization of rhythm-generating areas in the transverse plane in the neonatal rat. This model also cooperates with the distribution of sulforhodamine-labeled cells, which were found predominately in the medial intermediate gray matter and around the central canal, with few cells in the more lateral areas (Kjaerulff et al., 1994).

Pathways mediating rostrocaudal alternation

Both the lateral and the ventral funiculi contain pathways mediating rostrocaudal alternation. That lateral white fiber tracts can mediate rostrocaudal coordination has been demonstrated previously in the lamprey (Cohen, 1987) and in the chick embryo (Ho and O'Donovan, 1993). However, the present study provides the first indication that this role can be fulfilled by the ventral funiculus alone. In the lamprey, the median white matter is not sufficient to support coordination across the lesion, and in the chick, the ability of the isolated ventral funiculus to mediate rostrocaudal coordination has not been specifically investigated. The wide cross-sectional area covered by the pathways mediating rostrocaudal alternation leaves the impression that the pathways coordinating locomotor-related activity in the newborn rat are redundant.

Rhythm-generating capability and pathways coordinating bilateral activity along the rostrocaudal axis of the cord

Using a split-bath set-up with a rostral and caudal pool and restricted longitudinal lesioning, Cazalets and coworkers (1995) concluded that the spinal rhythm generator in the neonatal rat and the pathways responsible for left/right alternation are restricted to the L1–L2 segments. Our results contradict such an absolute statement. First, rhythmic bursting could be obtained in segments caudal to L2 and rostral to L1. Second, we found that significant left/right alternation was preserved with the Th12–L2 segments split midsagitally. Therefore, our results suggest that the rhythm-generating capability and the fibers responsible for left/right alternation are distributed along the entire length of the lumbar spinal cord and also extend into the caudal thoracic segments (see Fig. 10). Previous reports in the neonatal rat support these conclusions. In a preliminary report, Kudo and Yamada (1987) demonstrated that a midline-hemisected L4–L5 preparation could produce alternating EMG activity in antagonist hindlimb muscles. In addition, left/right and flexor/extensor phase relationships are maintained after midsagittal sections of the L1–L6 segments in C1–L6 preparations (Cowley and Schmidt, 1993). Also, in strychnine-treated preparations in which left/right alternation is transformed into synchrony, any one segment in the cord is sufficient to keep this synchrony (K. C. Cowley and B. J. Schmidt, personal communication). On the other hand, it is also clear that the rostral lumbar segments (L1–L2) have a higher rhythm-generating (and coordinating) capability than the caudal lumbar segments (Table 1). Such a rostrocaudal

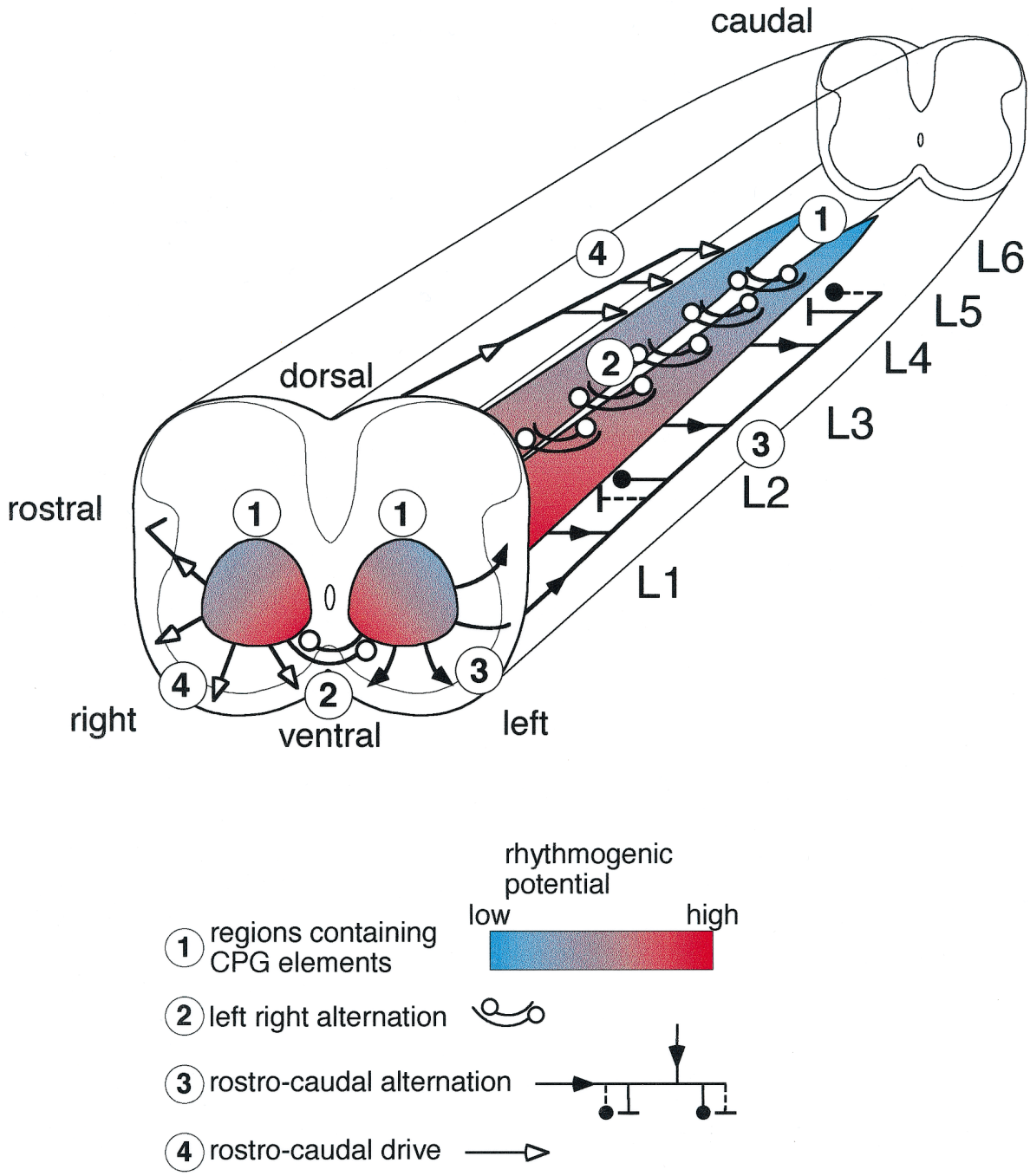

Figure 10. Summary of the lesion experiments. The rhythm-generating network in L1–L6 is shown distributed along the cord as two medial columns (*1*). The taper and the color gradient indicate the high rostral and lower caudal ability to generate rhythmic activity. In the rostral end, the columns are shown in cross section, indicating that the rhythmogenic networks extend rostrally into the thoracic segments. The area below the level of the central canal almost with certainty contains part of the CPG for locomotor-related rhythmicity in the newborn rat. The neighboring upper area lateral and dorsal to the central canal also is likely to contain rhythm-generating networks, although this was not proven directly in this study. The mediolateral color gradient indicates the lower rhythmogenic potential in the lateral direction. The localization of the pathways mediating left/right alternation in the ventral commissure is indicated (*2*). The pathways mediating rostrocaudal alternation are shown widely distributed in the lateral and ventral funiculus on the left side of the preparation (*3*); note the possible contribution from all levels along the rostrocaudal axis. The rostrocaudal drive is indicated on the right side of the cord (*4*).

gradient for the regions controlling hindlimb rhythmicity (indicated in Fig. 10 by the taper of the CPG columns) is a general phenomenon in quadropedial vertebrates and has been demonstrated in turtle (Mortin and Stein, 1989), cat (Deliagina et al., 1983; Arshavsky et al., 1984; Gelfand et al., 1988), and chick (Ho and O'Donovan, 1993). Presently, there is no explanation for this rostrocaudal gradient in the ability to generate rhythmicity. Furthermore, we do not have a clear-cut explanation for the discrepancy between Cazalets et al. (1995) and our observations on the distribution of rhythmogenic potential along the

cord. The most obvious differences between the two experimental situations are that we used considerably lower transmitter concentrations to induce locomotion than did Cazalets et al. (1995). Because preliminary results in the present study suggest that high transmitter concentrations decrease reciprocal inhibition, it is possible that application of high transmitter concentrations to caudal segments (where the reciprocal inhibitory connections appear to be weaker than rostral segments) will result in tonic activity, and thus the failure to see rhythmic activity. Alternatively, the differences are age-related. This study used 0- to 2-d-old animals, whereas Cazalets et al. (1995) used 1- to 4-d-old animals. In embryonic chick, it has been shown that the rostral lumbosacral cord generates more cycles of rhythmic activity than the caudal part of the cord, and this difference becomes more pronounced with development (Ho and O'Donovan, 1993). It is possible that a similar rostralization takes place in the postnatal rat.

The distribution along the cord of the rhythmogenic capability as it appears from the lesion experiments fits well with the density of sulforhodamine-labeled cells at various rostrocaudal levels (Kjaerulff et al., 1994). First, labeled cells appeared in the caudal thoracic segments. Second, the rostral-to-caudal gradient in rhythmogenic potential (Table 1) might correspond to the higher labeling density in the L1–L2 and L3–L4 double segments than in L5–L6.

Our results have shown that intact connections to rostral segments increase the modulation amplitude of rhythmic bursting in caudal segments. This suggests, as indicated in Figure 10, that the caudal rhythm generators are supported by a drive from rostral centers as also suggested by Cazalets et al. (1995).

Finally, our study has revealed that axons responsible for the left/right alternation are restricted to the ventral commissure (see Fig. 10). This localized crossing might provide an important experimental tool in future experiments aimed at identifying those CPG neurons generating the reciprocal inhibition between the two sides of the cord.

REFERENCES

Arshavsky Y, Gelfand IM, Orlovsky GN, Pavlova GA, Popova LB (1984) Origin of signals conveyed by the ventral spino-cerebellar tract and spino-reticulo-cerebellar pathway. Exp Brain Res 54:426–431.

Baev KV (1978) Periodic changes in primary afferent depolarization during fictitious locomotion in thalamic cats. J Neurophysiol 10:316–317.

Barajon I, Gossard JP, Hultborn H (1992) Induction of *fos* expression by activity in the spinal rhythm generator for scratching. Brain Res 588:168–172.

Batschelet E (1981) Circular statistics in biology (Sibson R, Cohen JE, eds). New York: Academic.

Cazalets JR, Sqalli-Houssaini Y, Clarac F (1992) Activation of the central pattern generators for locomotion by serotonin and excitatory amino acids in neonatal rat. J Physiol (Lond) 455:187–204.

Cazalets JR, Borde M, Clarac F (1995) Localization and organization of the central pattern generator for hindlimb locomotion in newborn rats. J Neurosci 15:4943–4951.

Cohen A (1987) Effects of oscillator frequency on phase-locking in the lamprey central pattern generator. J Neurosci Methods 21:113–125.

Cowley KC, Schmidt BJ (1993) Effects on locomotor rhythm of acute transverse and midsagittal lesions of the *in vitro* neonatal rat spinal cord. Soc Neurosci Abstr 19:540.

Cowley KC, Schmidt BJ (1995) Effects of inhibitory amino acid antagonists on reciprocal inhibitory interactions during rhythmic motor activity in the in vitro neonatal rat spinal cord. J Neurophysiol 74:1109–1117.

Dai X, Douglas JR, Nagy JJ, Noga BR, Jordan LM (1990) Localization of spinal neurons activated during treadmill locomotion using the *c-fos* immunohistochemical method. Soc Neurosci Abstr 16:889.

Delcomyn F (1980) Neural basis of rhythmic behavior in animals. Science 210:492–498.

Deliagina TG, Orlovsky GN, Pavlova GA (1983) The capacity for generation of rhythmic oscillations is distributed in the lumbosacral spinal cord of the cat. Exp Brain Res 53:81–90.

Dubuc R, Cabelguen JM, Rossignol S (1985) Rhythmic antidromic discharges of single primary afferents recorded in cut dorsal root filaments during locomotion in the cat. Brain Res 53:81–90.

Durand GM, Kovalchuk Y, Konnerth A (1996) Long-term potentiation and functional synapse induction in developing hippocampus. Nature 381:71–75.

Gelfand IM, Orlowsky GN, Shik ML (1988) Locomotion and scratching in tetrapods. In: Neural control of rhythmic movements in vertebrates (Cohen AH, Rossignol S, Grillner S, eds), pp 285–332. New York: Wiley.

Grillner S (1981) Control of locomotion in bipeds, tetrapods and fish. In: Handbook of physiology, Sec 2, The nervous system (Brookhardt JM, Mountcastle VB, eds), pp 1179–1236. Bethesda, MD: American Physiological Society.

Grillner S, Zangger P (1979) On the central generation of locomotion in the low spinal cat. Exp Brain Res 34:241–261.

Ho J, O'Donovan MJ (1993) Regionalization and intersegmental coordination of rhythm-generating networks in the spinal cord of the chick embryo. J Neurosci 13:1354–1371.

Kiehn O, Kjaerulff O (1996) Spatiotemporal characteristics of 5-HT and dopamine-induced rhythmic hindlimb activity in the *in vitro* neonatal rat. J Neurophysiol 75:1472–1582.

Kiehn O, Johnson BR, Raastad M, Kjaerulff O (1995) Synaptic inputs to and active membrane properties of spinal interneurons during chemically induced rhythmicity in the isolated neonatal rat spinal cord. Soc Neurosci Abstr 21:152.

Kiehn O, Johnson BR, Raastad M (1996) Plateau potentials in mammalian spinal interneurons during transmitter-induced locomotor activity. Neuroscience, in press.

Kjaerulff O, Kiehn O (1994) Localization of the central pattern generator for hindlimb locomotion in the neonatal rat. A lesion study. Soc Neurosci Abstr 20:1757.

Kjaerulff O, Kiehn O (1995) Rostro/caudal and left/right coordination of rhythmic activity in the lumbar spinal cord of the newborn rat *in vitro*. Neurons, Networks, and Motor Control Symposium, Nov. 8–11, 1995, Tucson, AZ.

Kjaerulff O, Barajon I, Kiehn O (1994) Sulphorhodamine-labelled cells in the neonatal rat spinal cord following chemically induced locomotor activity *in vitro*. J Physiol (Lond) 478:265–273.

Kudo N, Yamada T (1987) *N*-methyl-D,L-aspartate-induced locomotor activity in a spinal cord-hindlimb muscle preparation of the newborn rat studied *in vitro*. Neurosci Lett 75:43–48.

MacLean JN, Hochman S, Magnuson DSK (1995) Lamina VII neurons are rhythmically active during locomotor-like activity in the neonatal rat spinal cord. Neurosci Lett 197:9–12.

Molander C, Xu Q, Grant G (1984) The cytoarchitectonic organization of the spinal cord in the rat. I. The lower thoracic and lumbosacral cord. J Comp Neurol 230:133–141.

Mortin LI, Stein PSG (1989) Spinal cord segments containing key elements of the central pattern generators for three forms of scratch reflex in the turtle. J Neurosci 9:2285–2296.

O'Donovan M, Ho S, Wayne Y (1994) Calcium imaging of rhythmic activity in the developing spinal cord of the chick embryo. J Neurosci 14:6354–6369.

Smith JC, Feldman JL (1987) In vitro brainstem-spinal cord preparations for study of motor systems for mammalian respiration and locomotion. J Neurosci Methods 21:321–333.

Sqalli-Houssaini Y, Cazalets JR Clarac F (1993) Oscillatory properties of the central pattern generator for locomotion in neonatal rats. J Neurophysiol 70:803–813.

Viala D, Buisseret-Delmas C, Portal JJ (1988) An attempt to localize the lumbar locomotor generator in the rabbit using 2-deoxy-[^{14}C]glucose autoradiography. Neurosci Lett 86:139–143.

Wheatley M, Jovanovic K, Stein RB, Lawson V (1994) The activity of interneurons during locomotion in the *in vitro Necturus* spinal cord. J Neurophysiol 71:2025–2032.

Zar JH (1974) Circular distribution. In: Biostatistical analysis (McElroy WD, Swanson CP, eds), pp 310–327. Englewood Cliffs, NJ: Prentice-Hall.